revista Matéria

ISSN 1517-7076

Revista Matéria, v. 13, n. 4, pp. 579 – 586, 2008
http://www.materia.coppe.ufrj.br/sarra/artigos/artigo11002

Structural analysis and shape-dependent catalytic activity of Au, Pt and Au/Pt nanoparticles

Esparza, R.[I]; Rosas, G.[II]; Valenzuela, E.[III]; Gamboa, S.A.[III]; Pal, U.[IV]; Pérez, R.[I];

[I] Instituto de Ciencias Físicas, Universidad Nacional Autónoma de México, P. O. Box 48-3, Cuernavaca, Mor., 62251, Mexico.
e-mail: resparza@ce.fis.unam.mx, ramiro@fis.unam.mx

[II] Instituto de Investigaciones Metalúrgicas, UMSNH, Edificio U, Ciudad Universitaria, Morelia, Mich., 58000, Mexico.
e-mail: grtrejo@jupiter.umich.mx

[III] Centro de Investigación en Energía, Universidad Nacional Autónoma de México, Temixco, Mor., 62580, Mexico.
e-mail: eevm@cie.unam.mx, sags@cie.unam.mx

[IV] Instituto de Física, Universidad Autónoma de Puebla, Apdo. Postal J-48, Puebla, Pue., 72570, Mexico.
e-mail: upal@sirio.ifuap.buap.mx

ABSTRACT

Metallic nanoparticles of Au, Pt and Pt/Au have been synthesized using a chemical reduction approach. The structural characterization of these metallic nanoparticles has been carried out using conventional transmission electron microscopy (TEM) and high resolution transmission electron microscopy (HR-TEM) techniques. HR-TEM images of Pt nanoparticles reveal their fcc-like structures, in the [103] and [011] orientations. However, in case of Au, the main structures are fcc-like and decahedral morphologies with five-fold symmetry axes. The structure of the gold nanoparticles was verified through their theoretically-simulated images, using a multislice approach of the dynamical theory of electron diffraction. These small particles have been used as electrocatalysts in Nafion membranes for fuel cell applications. The electrochemical characterization of the membranes shows that the Pt dispersion gives best performance for fuel cell applications.

Keywords: gold, platinum, nanoparticles, chemical reduction synthesis, electron microscopy, structural determination, electrochemical characterization.

1 INTRODUCTION

During the last decade, due to the emergence of a new generation of materials with technological applications, the number of groups involved in nanomaterial research has been increased exponentially [1]. Nanomaterials are related with several scientific and technological domains such as chemistry, electronics, high density magnetic recording media, sensors and biotechnology. This, in part, is due to their novel properties that differ from both the isolated atoms and the bulk [2]. An ultimate challenge in materials research is now the creation of perfect nanometer-scale (in size and shape) crystallites, identically replicated in unlimited quantities which can be handled as easily as bulk materials.

Colloidal solutions favor partial control of the size and shape of nanomaterials. Several techniques have been utilized to produce amorphous and crystalline nanomaterials by soft chemistry. Whatever the procedure is, the major factors involved in controlling the size and shape of nanoparticles are the concentration of reactants, electrostatic interactions between the nanoparticles and surfactants, and reactant solubility in the solvent. For technological applications, it is important to develop nanoparticle dispersions without aggregation or coalescence. After or during synthesis, the nanoparticles need to be passivated to prevent coalescence. A lesser amount of surfactant than the optimum, in which the surfactant doesn't perfectly cover the entire surface of the particles, can cause coalescence of the particles or uncontrolled increasing in particle size. On the other hand, excess amount of surfactant may cause aggregation of the particles through bridging between the surfactant molecules (generally some organic polymers). When an excess amount of surfactant/dispersant is added, the amount of non-adsorbed dispersant molecules increase in the solvent and, due to depletion effect, the coalescence of the particles can be promoted. One of the first

Autor Responsável: Esparza, R. Data de envio: 22/11/2007 Data de aceite: 28/03/2008

approaches to make nanoparticles was based on the variation of the solubility product of reactant with temperature [3]. This controls the particle size. Simultaneously, synthesis of nanoparticles was developed in aqueous solution in presence of charged polymers that strongly interact with one of the reactants [4, 5].

Polymer-embedded metallic nanoparticles have been extensively studied [6]. Because of unique physical characteristics, metal–polymer nanocomposites are potentially useful for a number of advanced functional applications, especially in the optical, catalysis and photonic fields. In particular, these materials can be used as light-stable color filters [7], polarizers [8, 9], ultra-low refractive index materials [10], nonlinear optical devices [11], optical sensors [12], and so on. However, the chemical routes that allow us to obtain monodispersed metallic nanoparticles with controlled size are still limited. The morphology and stability of the nanoparticles depend on the precursors, their concentration, and the type of the reducing agent [13].

In this work we report the synthesis of Pt, Au, and AuPt nanoparticles by a chemical reduction method, which generates clusters in the range of 1–10 nm. The nanoparticles have been characterized by using TEM and HR-TEM. Simulated HR-TEM images were used to identify the structures of the nanoparticle obtained experimentally. The electrochemical characterizations of the proton conducting membranes impregnated with nanoparticles are performed to verify their applications in fuel cells.

2 EXPERIMENTAL PROCEDURE

2.1 Synthesis

The metallic nanoparticles have been obtained using a chemical reduction method. Methanol solutions of Au and Pt ions were prepared by dissolving the corresponding metallic salts ($HAuCl_4 \bullet xH_2O$, $HPtCl_6 \bullet 6H_2O$) in methanol. The solutions were mixed in desired volumetric ratios for the preparation of bimetallic ion mixtures. A methanol solution of PVP [poly (N-vinyl-2-pyrrolidone)] was added to the metal ion mixtures. To reduce the metal ions, 6 mL aqueous solution of $NaBH_4$ (0.066 M) was added to the mixture solution drop wise at room temperature. A homogeneous colloidal dispersion was produced after the addition of $NaBH_4$ reductor in the solution containing metal ions. The details of the synthesis process have been discussed in ref. [14].

2.2 Microstructural Characterization

The structural and morphological characteristics of the dispersed metallic nanoparticles have been studied using a Philips Tecnai F20 transmission electron microscope, which has a field emission gun attachment, an operating voltage of 200 keV, a spherical aberration of 1 mm, and a direct maximum resolution dot to dot of 0.23 nm. TEM specimens were prepared by dispersing and subsequent drying a drop of colloidal solutions on a copper grid (3 mm in diameter) covered with an amorphous carbon film. The HR-TEM images obtained have been digitally processed.

2.3 Theoretical Approaches

Theoretical simulations based on the multislice approach of the dynamical theory of electron diffraction [15] have been carried out to generate HR-TEM images of gold nanoparticles. The multislice method is based on the physical optics approach [16]. The crystal of thickness z is sliced into many thin slices of small thickness Δz. For each slice the crystal potential is projected onto a plane (usually the entrance plane of the slice) and introduces a modulation the transmittance of the slice (this is equivalent to assume that the scattering of the incident wavefront by the crystal potential of each thin slice is entirely located on the plane of projection). The propagation of the modified wavefront to the next slice is done in vacuum over the very small distance Δz. Its physical optics equivalent is described by the Fresnel approximation of the Rayleigh-Sommerfeld diffraction formula [16], where the object is replaced by an infinite number of point sources emitting spherical wavelets with their complex amplitude given by the product of the incident wavefront by the transmittance of the object.

2.4 Electrochemical Characterization

Nafion® 115 membranes (Dupont) were impregnated with Au, Pt and Au/Pt nanoparticles by immerging them into the corresponding colloidal solutions for about 1 h. These membranes were activated in 1M H_2SO_4 solution for 48 h. A membrane-electrode assembly (MEA) with double diffusing layer in the anode (carbon cloth and paper) and a layer in the cathode (carbon cloth) was prepared for electrochemical

evaluation. A new MEA with a commercial Pt electrocatalyst (Electrochem Inc) was performed. In this case, 0.4 mgr/cm^2 of Pt was deposited on carbon Vulcan. Liquid Nafion 115 (5%) was added to improve the contact between the membrane and the electrocatalyst. The electrocatalyst was applied by the brushing technique. Later the diffusing layers (carbon cloth) were placed. All the membrane-electrode assemblies were placed between two aluminum plates at 150 ºC and were pressed to100 kg/cm^2. The flow of reactant gases (H_2 and O_2) was 30 cm^3/min for both. The MEA's were characterized in a fuel cells system (ElectroChem). The used configuration was like a polymer electrolyte membrane fuel cell (PEMFC). The protonic conductivity (I-V curves) of the impregnated membrane was measured with the 4 electrodes method. The values obtained for the impregnated membranes and a commercial membrane were compared.

3 RESULTS AND DISCUSSION

Utilizing the chemical reduction method, metallic nanoparticles in an extensive size range could be produced [14, 17]. As the colloidal solutions prepared usually contain particles of different sizes, it is necessary to obtain their average size and size distribution before applying them in a membrane-electrode assembly (MEA). Figure 1 shows a typical TEM image of the Pt nanoparticles produced. Formation of dispersed Pt nanoparticles of uniform size can be observed. From the size distribution histogram (inset), an average particle size of 2.1 ± 0.2 nm could be estimated. About 500 nanoparticles were considered for each sample to obtain their size distribution histograms.

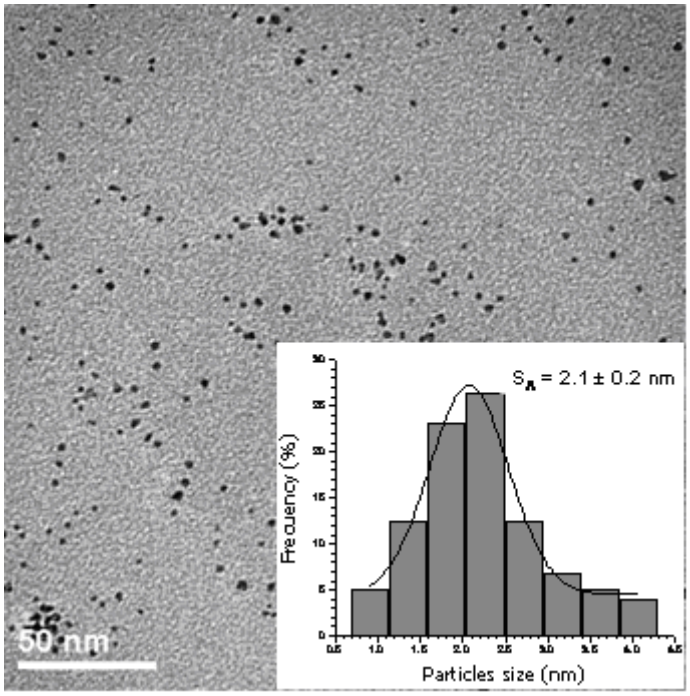

Figure 1: A typical TEM image of the Pt nanoparticles with size distribution histogram.

A small size distribution exists for all the samples. The particle size distribution for all the colloidal solutions is illustrated in Figure 2. While for pure Pt, the average particle size is about 2.1 nm with small dispersion in size, for pure Au the average particle size is about 1.7 nm with even less size dispersion. The size distributions for the Au/Pt (1:1) and Au/Pt (3:1) colloidal particles reveal average particle sizes of 2 nm and 1.8 nm, respectively. It is interesting to note that even when the Au/Pt (1:1) sample reveals a higher average particle size, there are still about 15% smaller particles (<1 nm).

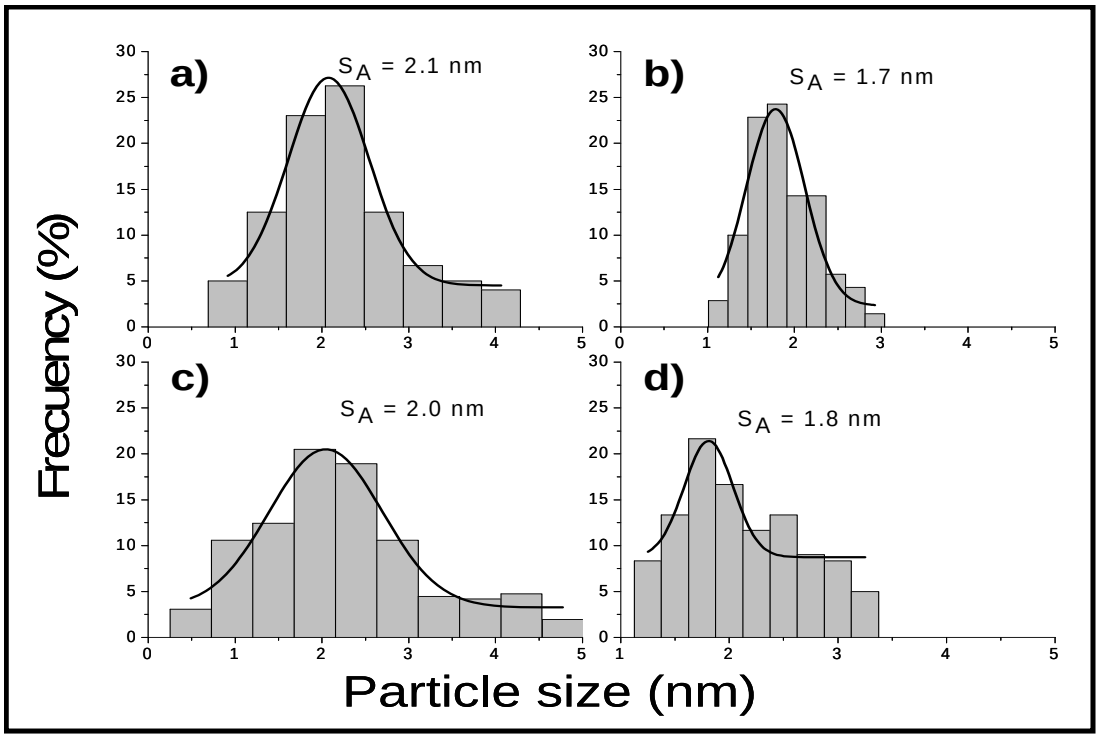

Figure 2: Size distribution histograms and corresponding average particle sizes for the Au/Pt nanoparticles of different compositions: a) Pt, b) Au, c) Au/Pt (1:1) and d) Au/Pt (3:1).

Figure 3 presents a sequence of HR-TEM images of three different samples: Pt, Au and Au/Pt in molar ratio 3/1. The Pt nanoparticle presented in Figure 3a is of fcc-like type with d-spacing of 0.195 nm, corresponding to (020) plane of Pt, and oriented in the [103] zone axis. These types of particles are very frequent in this sample. On the other hand, fcc-like and decahedral structures are frequently observed for the case of the Au nanoparticles. A decahedral nanoparticle oriented along its five-fold symmetry axis is clearly observed in the Figure 3b. Other types of structures were found in the other samples. For instance, single twin nanoparticles (stp) are observed in the case of Au/Pt with the different molar relations (1/1 and 3/1) (Figure 3c). The formation of twinned particles is very common for the transition metals with fcc crystal lattice when their size reduces to nanometer scale. Twinning often has a serious effect on the shape and symmetry of a nanocrystal, in particular, in the case of repeated twinning. Two types of repeated twinning are known: lamellar and cyclic. Lamellar twinning is characterized by parallel contact twins repeating continuously one after another, like single twin particles. Cyclic twinning requires nonparallel coplanar composition planes, like multiple twin particles (decahedron and icosahedron).

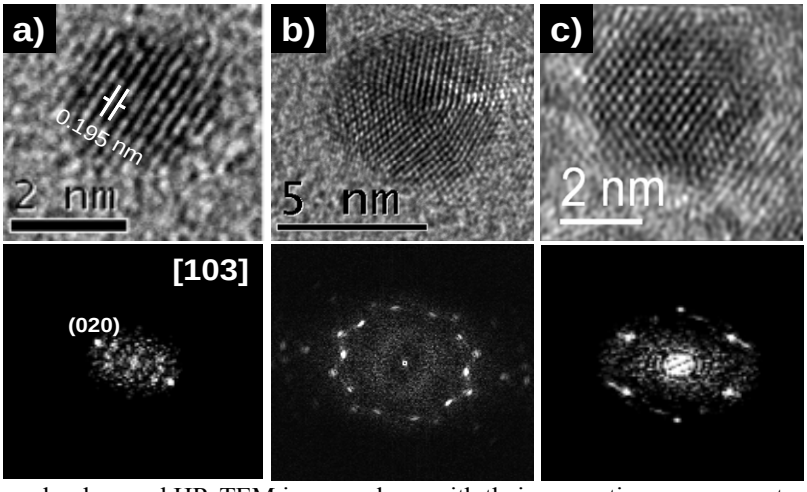

Figure 3: Commonly observed HR-TEM images along with their respective power spectra (at the bottom): a) Pt, b) Au and c) AuPt (3/1).

The structural morphology of metallic nanoparticles is strongly dependent on their stoichiometry. This is illustrated in Figure 4, where the frequency of the structural shapes as a function of nominal composition is displayed. In Figure 4, cubic (fcc), cubic with deformation (fccd), decahedral (deca), multiple twin particles (mtp), single twin particles (stp), and highly deformed particles (hdp) are the main structural configurations of the clusters. The Pt particles show fcc-like structural morphologies only. However, the Au particles have fcc-like and decahedron-like shapes. The Au/Pt (1:1) sample shows fcc-like and multiple twinned particles, and finally the Au/Pt (3:1) composition shows decahedron-like and twinned particles. Such structural evolutions involve multiple factors and the most important is related to the surface energy minimization, which is clearly higher for the pure Pt. In fact, the existence of twin clusters for the nanoparticles implies an internal strain, which is released to the defects present in them.

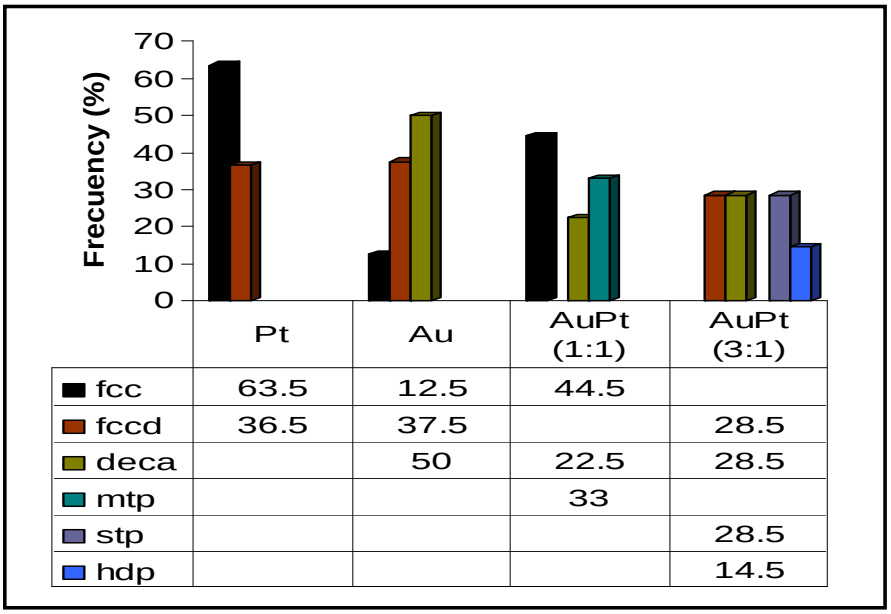

	Pt	Au	AuPt (1:1)	AuPt (3:1)
fcc	63.5	12.5	44.5	
fccd	36.5	37.5		28.5
deca		50	22.5	28.5
mtp			33	
stp				28.5
hdp				14.5

Figure 4: Distribution of different structural morphologies for the metallic nanoparticles. These distributions are obtained by analyzing several HR-TEM images of each of the samples. The notations for different morphologies are: fcc-like (fcc), fcc-deformed (fccd), decahedral (deca), multiple twin particle (mtp), single twin particle (stp) and highly-deformed particle (hdp).

Simulation of HR-TEM images is a useful method to understand the contrast of the experimental image, to examine if the resolution of an electron microscope is sufficiently high to solve a problem, and to determine the experimental conditions under which the images were obtained. In this study, simulated HR-TEM images were used to compare with the experimental images. Although mainly the truncated octahedron (fcc-like) nanoparticles are considered for simulation, a few of them are of different structural shapes, which were observed experimentally (presented in Figure 3b). Figure 5 shows the simulated HR-TEM image of an Au nanoparticle, where the multiple twinning domains with five-fold symmetry axis are identified. The twinning boundaries are coherent and free of defects such as dislocation or micro-twinning. The angle among the adjacent boundaries varies from 71.5 to 72.5º. This structure corresponds to a Marks decahedron, which varies with respect of the others (pentagonal bipyramid and Ino) mainly in the five-fold symmetry axis, due to the truncation of its vertexes.

Figure 6 shows an icosahedral type Au nanoparticle (Figure 6a) and its corresponding simulated image (Figure 6b). The orientation of the nanoparticle is difficult to be analyzed. However, the simulation technique allows us to identify all the possible orientations of the model. It is important to mention that due to different orientations of the particle, there should have differences in its image contrast profiles, which make it difficult to recognize an icosahedron from its experimentally obtained HR-TEM image. Simulated images are required for definitive identification of the different orientations observed. The icosahedral particles oriented along the two-fold symmetry axes are more frequently observed. In contrast, the five-fold symmetry axes are rarely observed. However, orientations near to the five-fold symmetry axes can be observed, as shown in Figure 6, where the icosahedron is rotated 3º along the five-fold symmetry axes. This is the characteristic of the Au nanoparticles and is associated with the interaction between the particles, the

amorphous carbon film, and high internal strains in the nanoparticles. In other metallic clusters such as silver, perfect five-fold symmetry axes have been observed [18].

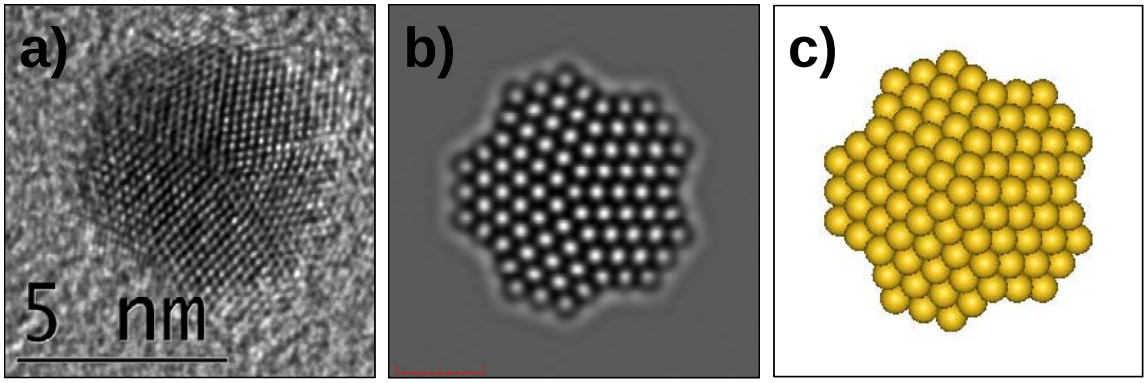

Figure 5: a) HR-TEM image of a decahedral gold particle, b) theoretically-simulated image of a decahedron along the five-fold symmetry axis, and c) model of the Marks decahedron.

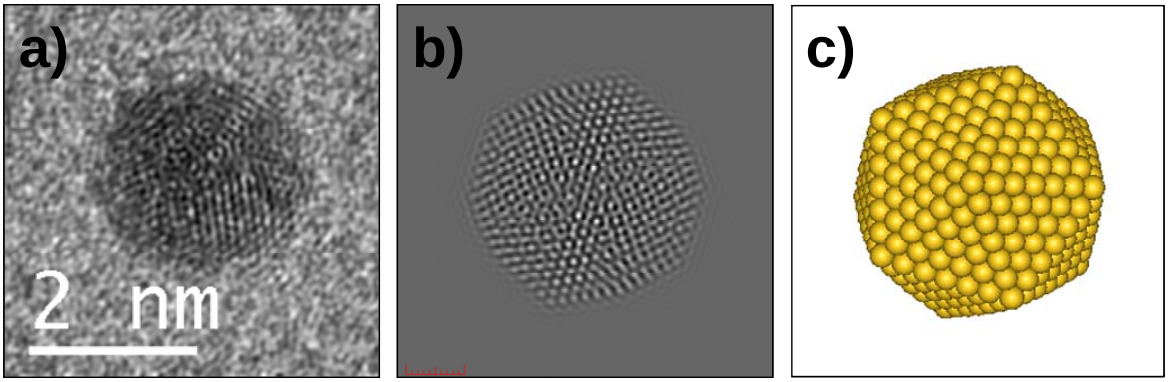

Figure 6: a) HR-TEM image of an icosahedral gold particle, b) theoretically-simulated image of an icosahedron near to the five-fold symmetry axis, and c) model of the icosahedron.

The metallic nanoparticles are frequently used for electrocatalytic applications. It has been shown that adding an extra diffusing layer in the anode (carbon cloth and paper) increases the value of the fuel cell current density [19] due to a better distribution of the reactants through the pores in the paper. An additional increment in the cell current density was obtained upon removing the paper diffusing layer of the cathode (only carbon cloth diffusing layer), which helps to store water in the membrane for long-term performance. The proton transport carries water along (water drag), while carrying the current. The water concentration gradient results in back diffusion. However, for operation at high current, the anode side of the membrane must be humidified to avoid dehydration. On the other hand, the water produced should be removed from the cathode side through an air stream to prevent flooding of the active layer. These actions allow us to have more sites for the oxygen reduction [19]. Figure 7 shows the performance of an electrochemical cell with the MEA impregnated with Pt, Au and Au/Pt nanoparticles in different molars relations (1/1, 1/3 and 3/1). Hydrogen and oxygen were used as test gases in the cell. It has been seen that the MEA impregnate with Pt gives the best electrocatalytic behavior [20]. However, the I-V curve for the MEA impregnate with Au/Pt (1/1) (red curve in Figure 7) is very similar to the MEA impregnated with Pt nanoparticles. It must be remembered that the main structure of Au/Pt (1/1) nanoparticles is MTP (multiple twinning particles) type, which indicate that the catalytic activity depends strongly on the structural type. On the other hand, the MEA impregnated with Au/Pt (3/1) has inferior electrocatalytic behavior to AuPt (1/1) impregnated MEA. The improvement in the catalytic activity of the bimetallic Au/Pt nanoparticles can be explained by the change in the electronic structure of the nanoparticles due to their changed morphology. The results obtained of the impregnated membranes with nanoparticles are compared with a commercial membrane with Pt catalyst (brown curve in Figure 7). The cell power generated by the commercial membrane was bigger to the obtained with impregnated membranes with colloidal nanoparticles. This is because the immersion time of the membranes in the colloidal solution was too much, causing that the nanoparticles penetrated in the

membrane, where they become inactive, because they are surrounded of Nafion polymer, which impedes that they are on contact with the hydrogen and the oxygen. However this technique is investigating yet, because this method application (immersion in the colloidal solution) is attractive to be economic, it does not require of special equipment, also, the variables are easy to control.

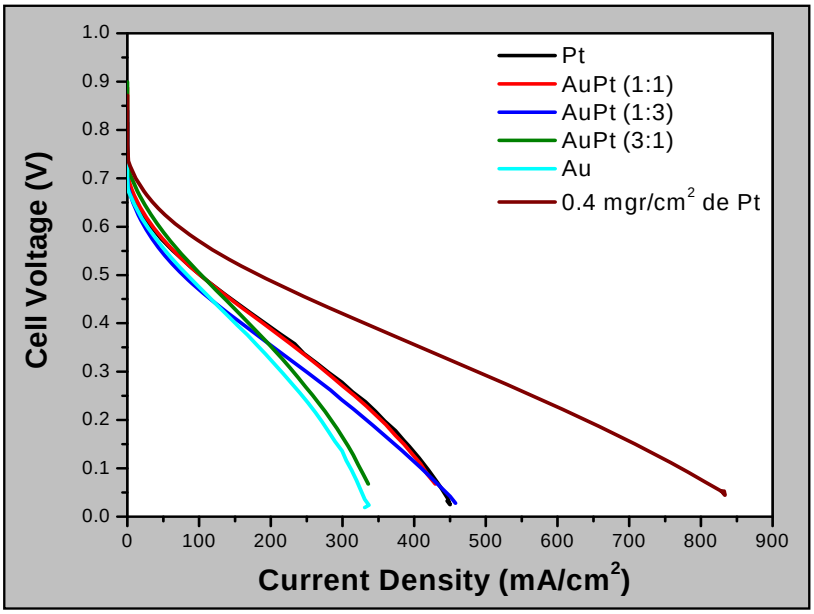

Figure 7: I-V curves for the assembles prepared with membranes impregnated with nanoparticles of Au and Pt in different proportions.

4 CONCLUSIONS

The synthesis method herein reported allows us to prepare metal nanoparticles with narrow size distributions. The main structures found were fcc-like for pure Pt, decahedral for pure Au, and single and multiple twinned structures for AuPt bimetallic particles. These structures influence the electrocatalytic behavior of MEA like Nafion. Therefore, the efficiency of polymer electrolyte membrane fuel cells (PEMFC) depends on the particle size, composition, and the structure of the electrocatalytic nanomaterials.

5 ACKNOWLEDGMENTS

We would like to acknowledge the technical support of A. Medina, C. Angeles-Chávez and A. Aguilar for the high-resolution electron microscopy.

6 BIBLIOGRAPHY

[1] MAMALIS, A.G., "Recent advances in nanotechnology", *Journal of Materials Processing Technology*, v. 181, pp. 52-58, 2007.

[2] JOSÉ-YACAMAN, M., ASCENCIO, J.A., LIU, H.B., GARDEA-TORRESDEY, J., "Structure shape and stability of nanometric sized particles", *Journal of Vacuum Science and Technology B*, v. 19, pp. 1091-1103, 2001.

[3] BRUS, L.E., "A simple model for the ionization potential, electron affinity, and aqueous redox potentials of small semiconductor crystallites", *Journal of Chemical Physics*, v. 79, pp. 5566-5571, 1983.

[4] HENGLEIN, A., "Small-particle research: physicochemical properties of extremely small colloidal metal and semiconductor particles", *Chemical Review*, v. 89, pp. 1861-1873, 1989.

[5] FENDLER, J.H., "Atomic and molecular clusters in membrane mimetic chemistry", *Chemical Review*, v. 87, pp. 877-899, 1987.

[6] CAROTENUTO, G., NICOLAIS, L., "Nanocomposites, metal-filled", In: Mark, H.F. (ed), *Encyclopedia of Polymer Science and Technology*, New York, USA, Wiley & Sons, 2003.

[7] DE LEON, A.G., DIRIX, Y., STAEDLER, Y., *et al*, "Method for fabricating pixelated, multicolor Polarizing Films", *Applied Optics*, v. 39, pp. 4847-4851, 2000.

[8] LU, A.H., LU, G.H., KESSINGER, A.M., FOSS, C.A., "Dichroic thin layer films prepared from alkanethiol-coated gold nanoparticles", *Journal of Physical Chemistry B.*, v. 101, pp. 9139-9142, 1997.

[9] DIRIX, Y., DARRIBERE, C., HEFFELS, W., *et al*, "Optically anisotropic polyethylene-gold nanocomposites", *Applied Optics*, v. 38, pp. 6581-6586, 1999.

[10] GROSSO, D., BOISSIÈRE, C., SANCHEZ, C., "Ultralow-dielectric-constant optical thin films built from magnesium oxyfluoride vesicle-like hollow nanoparticles", *Nature materials*, v. 6, pp. 572-575, 2007.

[11] SHALAEV, V.M., MOSKOVITS, M., *Nanostructured materials cluster, composites, and thin films*, washington, DC, USA, ACS Books, 1998.

[12] SEO, J.T., YANG, Q., CREEKMORE, S., *et al*, "Evaluation of nonlinear optical properties of cadmium chalcogenide nanomaterials", *Physica E*, v. 17, pp. 101-103, 2003.

[13] BRONSTEIN, L.M., CHERNYSHOV, D.M., TIMOFEEVA, G.I., *et al*, "Interaction of polystyrene-block-poly(ethylene oxide) micelles with cationic surfactant in aqueous solutions. metal colloid formation in hybrid systems", *Langmuir*, v. 16, pp. 3626, 2000.

[14] ESPARZA, R., ASCENCIO, J.A., ROSAS, G., *et al*, "Structure, stability and catalytic activity of chemically synthesized Pt, Au and Au-Pt nanoparticles", *Journal of Nanoscience and Nanotechnology*, v. 5, pp. 641-647, April 2005.

[15] GÓMEZ, A., BELTRÁN DEL RÍO L.M., "SimulaTEM", *Revista Latinoamericana de Metalurgia y Materiales*, v. 21, pp. 46-50, 2001.

[16] COWLEY, J.M., MOODIE, A.F., "The scattering of electrons by atoms and crystals: A new theoretical approach", *Acta Crystallographica*, v. 10, pp. 609-619, October 1957.

[17] ESPARZA, R., ROSAS, G., LÓPEZ-FUENTES, M., *et al*, "Synthesis of gold nanoparticles with different atomic structural characteristics", *Materials Characterization*, v. 58, pp. 694-700, 2007.

[18] XING, X., DANELL, R.M., GARZÓN, I.L., *et al*, "Size-dependent fivefold and icosahedral symmetry in silver clusters", *Physical Review B*, v. 72, n. 8, pp. 081405-081405.4, August 2005.

[19] VALENZUELA-MONDACA, E., *Estudio de la interfase electrodo/electrolito de una celda de combustible del tipo PEM mediante la técnica de espectroscopia de impedancia*, Ph.D. Thesis, UNAM, México, D.F., 2006.

[20] NEERGAT, M., SHUKLA, A.K., GANDHI, K.S., "Platinum-based alloys as oxygen-reduction catalysts for solid-polymer-electrolyte direct methanol fuel cells", *Journal of Applied Electrochemistry*, v. 31, n. 4, pp. 373-378, April 2001.

[21] CHOI, S.H., LEE, S., KIM, S.J., *et al*, "Preparation of polymer-stabilized palladium–silver bimetallic nanoparticles by c-irradiation and their catalytic properties for hydrogenation of cis, cis-1,3-cyclooctadiene", ***Catalysis Letters,*** v. 105, pp. 59-65, 2005.